Title
SOOT PROFILES IN BOUNDARY LAYER FLAMES

Authors
Beier, R.A.
Pagni, P.J.

Publication Date
1981-12-01

Lawrence Berkeley Laboratory
UNIVERSITY OF CALIFORNIA

ENERGY & ENVIRONMENT
DIVISION

To be presented at the Nineteenth International Symposium on Combustion, Haifa, Israel, August 8-13, 1982

SOOT PROFILES IN BOUNDARY LAYER FLAMES

R.A. Beier and P.J. Pagni

December 1981

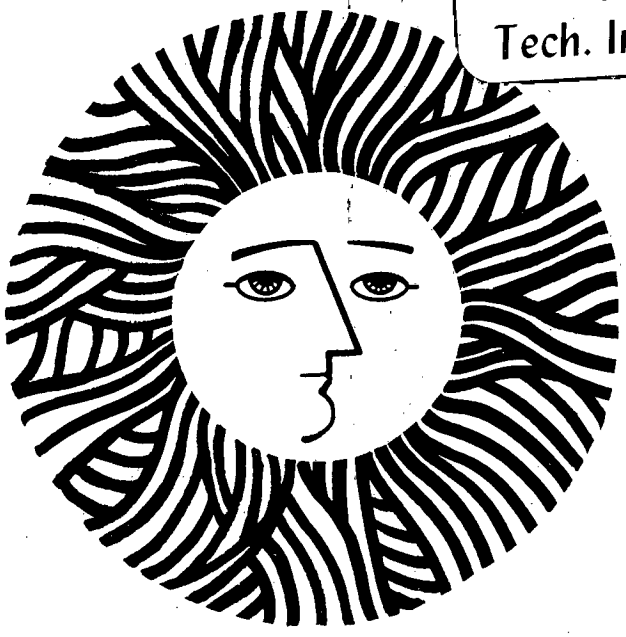

Prepared for the U.S. Department of Energy under Contract W-7405-ENG-48

DISCLAIMER

SOOT PROFILES IN BOUNDARY LAYER FLAMES

R.A. Beier* and P.J. Pagni

Lawrence Berkeley Laboratory

and

Mechanical Engineering Department

University of California

Berkeley, CA 94720

* Current address: Basic Research Department, Factory Mutual Research, 1151 Boston-Providence Turnpike, Norwood, Massachusetts 02062

Key Words: soot, fires, radiation, experimental methods

This work was supported by the U.S. Department of Energy under Contract No. W-7405-ENG-48; and by the Center for Fire Research in the U.S.D.O.C. National Bureau of Standards under Grant No. NB 80-NAG-E6839.

ABSTRACT

Carbon particulate volume fractions and approximate particle size distributions are measured in a free laminar combusting boundary layer for liquid hydrocarbon fuels (n-heptane, iso-octane, cyclohexane, cyclohexene, toluene) and polymethylmethacrylate (PMMA). A multiwavelength laser transmission technique determines a most probable radius and the total particle concentration, which are two parameters in an assumed form for the size distribution. In the combusting boundary layer, a sooting region exists between the pyrolyzing fuel surface and the flame zone. The liquid fuel soot volume fractions, f_v, range from $f_v \sim 10^{-7}$ for n-heptane, a paraffin, to $f_v \sim 10^{-5}$ for toluene, an aromatic. The PMMA volume fractions, $f_v \sim 5 \times 10^{-7}$, are approximately the same as the values previously reported for pool fires. The soot volume fractions increase with height; convection of carbon particles downstream widens the soot region with height. For all fuels tested, the most probable radius is between 20 nm and 50 nm, and it changes only slightly with height and distance from the fuel surface.

INTRODUCTION

In most fires thermal radiation is the dominant mode of heat transfer. Carbon particles within the flame are responsible for a large part of this emitted radiation and hence warrant quantification. Since a small, burning, vertical wall provides a two dimensional combusting boundary layer, which has been previously modeled,[1-3] this fire is chosen for study of flame soot. The volume fraction of soot and particulate size distributions are determined using a multiwavelength laser transmission technique.[4-8] In a steady, laminar, combusting boundary layer a pyrolysis zone separates a flame zone from the fuel surface as shown in Fig. 1. A layer on the fuel rich side of the blue flame zone is yellow, which indicates the presence of carbon particles. The width of the yellow soot layer increases with height. Our measurements determine the soot volume fraction at different heights in the combusting layer for five liquid hydrocarbon fuels and one solid fuel.

Minchin[9] and Clarke, Hunter, and Garner[10] did early studies of the effect of fuel type on soot formation in laminar diffusion flames. They increased the height of a flame on a small, circular burner by increasing the fuel flow rate until the flame emitted soot at its tip. This height is called the smoke height or sooting height. For comparing different fuels, a lower smoke point indicates a greater amount of soot formation. Recently, Glassman and Yaccarino[11] measured sooting heights to show the importance of flame temperature in addition to fuel structure. The results of the present experiment quantify the effect of fuel type on the amount of soot produced by hydrocarbon fuels. These results also provide

experimental bases for soot formation and destruction modeling by giving detailed profiles of soot volume fractions within the well characterized boundary layer.

Using a modified Schmidt Method technique, Markstein[12] determined absorption-emission coefficients and volume fraction of soot in pool fires. Pagni and Bard[4-7] determined the volume fraction of soot and particulate size distribustions in small pool fires. Jagoda, Prado, and Lahaye[13] measured local soot concentrations by probe and laser light scattering and absorption techniques in a candle-like diffusion flame. With these previous measurements, the results of the present study provide a comparision between soot volume fractions in a pool fire and a free flow boundary layer with the same fuel. Related experiments for gaseous fuels have been reported by Kent, Jander, and Wagner,[14] and Haynes, Jander, and Wagner,[15,16] and Chang and Penner.[17]

Sibulkin, Kulkarni, and Annamalai,[18] and Liu and Shih,[19] and Kinoshita, Pagni, and Beier[20,21] recently included radiation in models of a laminar combusting boundary layer. These models require a knowledge of the soot volume fraction within the layer, which is provided by the present study.

EXTINCTION ANALYSIS

The multiwavelength laser transmission technique is based on an extinction analysis, the details of which are described elsewhere,[4-7,22] so only a brief outline of the analysis and assumptions is given here. The transmitted intensity, I, of a monochromatic beam through a polydisperse aerosol is related to the

initial intensity, I_o by

$$I(\lambda)/I_o(\lambda) = \exp(-\tau(\lambda)L) \quad (1)$$

where L is the beam pathlength. An aerosol spectral extinction coefficient , τ , is given by

$$\tau(\lambda,mr) = \int_o^\infty N(r)\, Q(\lambda,m,r)\, \pi r^2 dr \quad (2)$$

where Q is the particle extinction efficiency from the Mie scattering theory[23] for spherical particles. Calculation of a spectral extinction coefficient requires knowledge of the optical properties of soot, m=n(1-ik), and the size distribution, N(r). The values of the optical properties which were derived by Lee and Tien[24] and listed by Bard and Pagni[5] are chosen over those reported by Dalzell and Sarofim.[25] A Gamma size distribution[26] with $\sigma/r_m = 1/2$, based on micrograph data obtained by Wersborg, Howard, and Williams,[27]

$$N(r)/N_o = (27\, r^3/2r_{max}^4) \exp(-3r/r_{max}) \quad (3)$$

is assumed, where r_{max} is the most probable radius, and N_o is the total particle concentration. The value of σ/r_m does not significantly affect f_v, although the value of r_{max} does change. The volume fraction of soot is defined by

$$f_v \equiv \frac{4}{3}\pi \int_o^\infty N(r)\, r^3 dr \quad (4)$$

which, with Eq. (3), gives

$$f_v = \frac{54\pi}{3^8}\, \Gamma(7)\, N_o r_{max}^3 = 18.62\, N_o r_{max}^3 \quad (5)$$

Measurements are made of the ratio of the transmitted and initial

intensities, I/I_o, at two different wavelengths, superimposed over the same pathlength, L. Substituting these measured values into equation (1) gives two independent values of τ, one at each wavelength. These two τ values give two independent Eqs. (2) to determine the two unknowns in the size distribution,[4-7] N_o and r_{max}. The volume fraction of soot is obtained from Eq. (5).

Since soot particles may agglomerate into larger clusters, Lee and Tien[28] studied how different shapes affect the radiative characteristics of a medium. With long chains approximated as cylinders, they considered spherical and cylindrical particles as two limiting cases. From their calculations, particle shape is most important in the far infrared region. For the visible wavelengths of these transmission measurements and the near infrared region of most flame radiation, calculations based on spherical particles give satisfactory results.

EXPERIMENTAL METHOD

The experimental setup, which is shown in Fig. 2, is similar to that described by Pagni and Bard.[5-7] Two lasers are used: a Spectra-Physics Argon Ion tunable laser model 165, operating at either λ = 0.4579 um, 0.4880 um, or 0.5145 um, and a Spectra-Physics Helium Neon laser model 125, emitting at λ = 0.6328 um. After a cube beam splitter superimposes the two beams from the lasers, the beams pass through the same physical space in the fire. A first simple lens reduces the diameter of the beams in the fire. After a second lens collects the transmitted light, an equilateral prism separates the two beams. Each beam passes through another focusing lens and a narrow band pass filter, before it strikes a laser power meter (Newport

Research Corp., model 820). The beam splitter provides a second beam from each laser, which is monitored as a reference intensity by the same prism-detector system. A PDP-11/34 microcomputer stores the data, after the output signals from the detectors pass through a d.c. amplifier and a (Digital Equipment Corp.) AR11 16-channel, 10 bit, A/D converter. A digital timer, with an adjustable period, triggers the A/D converter to read the output signals of the detectors.

The liquid fuel wick or the solid fuel sample is mounted in a small, vertical wall, which is bolted to a movable table. The inert wall is made of Marinite-XL (Johns-Manville Co.), and its width and height are 0.5 m. The wick, ceramic fiber board (Fiberfrax Hot Board, Carborundum Co.), has its front surface flush with the inert wall surface. With aluminum foil around the hidden surfaces of the wick, the inert wall does not absorb the liquid fuel.

Since the transmission of the laser beams varies greatly for the different fuels, wicks of different widths are used as listed in Table 1. The wicks are 12 cm high, except those used for the extremely sooty toluene are 6 cm high. The samples of PMMA are 15 cm high and 1.27 cm thick. The diameter of the laser beam in the flame limits the spatial resolution of the transmission measurement. For pathlengths of 16 cm and 7 cm the maximum beam width between points of $1/e^2$ intensity is less than 0.4 mm and 0.3 mm, respectively.

Since variations in temperature and species change the index of refraction in the direction normal to the fuel surface, the fire deflects the laser beam. The angular deflection of the beam in the combusting boundary layer is greater than the deflection from pool fires,[4-7] due to the steeper gradients in the species and temperature

profiles in the boundary layer. This angular deflection can change the physical pathlength of the beams through the prism and cause the beams to miss the detectors. Lens FL2 in Fig. 2 is used to minimize the beam movement relative to the prism and the detectors. The position of lens FL2 bisects the distance between the prism and the center of the fire, which is set at four times the focal length of lens FL2. This arrangement projects an image of the beam at the center of the fire onto the prism. Since the linear displacement of the beam is small at the center of the fire, the movement of the beam is small at the prism.

The deflection of the beam in the fire is measured for all the fuels. For liquid fuels the deflection does not decrease the spatial resolution significiantly except near the inner edge of the soot layer when the width of the wick is 15 cm. Therefore, data near the inner boundary of the soot layer are obtained from measurements with shorter pathlengths. Since the deflection of the beam is less for PMMA, a larger pathlength of 16 cm is used.

The distance between the superimposed laser beams and the fuel surface is changed by moving the fire horizontally. A complete scan of the fire is obtained by adjusting the height of the wall between traverses. After the fuel is ignited, a 0.4 m square sheet of pyrex glass is placed in front of the fire about 0.25 m from the fuel surface to block disturbances from air movements in the room. For liquid fuels the supply of fuel in the wick gives a steady flame for about five minutes after a very short transient period. This steady period allows one horizontal scan, with increments of $\sim$ 0.4 mm, through the boundary layer each time the fire is ignited. At each

position the outputs of the detectors are read 300 times within a 6 second interval. After each horizontal scan the fire is extinguished, the height of the wall is changed, and the wick is soaked with fuel before the fire is reignited.

For the liquid fuels the pathlength, L, is approximately 1 cm longer than the wick width. For PMMA beam pathlength is slightly less than the sample width, because near the sample edges the flame follows the round edges of the sample. The pathlength is taken as the length of the luminous zone as measured by placing a scale directly in front of the flame at the laser beam location. End effects may be neglected for these large L. The measured values of I/I_o for the two different wavelengths and L are used in the extinction analysis to calculate r_{max} and f_v. Data for more than one wavelength pair are used to isolate the correct value[4-7] of r_{max} and reduce any uncertainty due to optical properties.

For PMMA the fuel regression rate affect on the beam distance from the fuel surface was taken into account. The regression rate is measured by blocking the laser beams partially with the fuel surface. If the vertical wall remains stationary, the surface of the pyrolyzing fuel slab moves and blocks a smaller part of the laser beams. The regression rate is the rate the vertical wall is moved to maintain a constant reading of transmitted intensity for the partially blocked beam. The regression rate is measured before and after each horizontal scan through the boundary layer. A new sample of PMMA is burned for the transmission measurements at each height.

Due to some unsteadiness in the fire, the positions of the soot layer and the flame zone fluctuate. Near the boundaries of the soot zone, a point at a fixed distance from the fuel surface spends only part of the time in the soot layer. Likewise, only a part of the pathlength of the laser beam through the fire may be in the soot layer at any time. Since the measured pathlength is the entire width of the fire, transmission measurements near a boundary may give too high a value of I/I_o, i.e. too low an attenuation, and therefore, a lower volume fraction of soot than the true value. At the outer soot layer boundary the portion of the beam in the soot layer is visible from light which is scattered by the soot. Measurements made at positions where only a fraction of the beam is in the soot layer are deleted from the data. At the inner boundary an increase in the experimental standard deviations of the volume fraction of soot and the most probable radius occurs. On these bases data points are rejected where $\sigma_{f_v}/f_v > 0.4$. The increase in the length of the standard deviation bars in Figs. 4 through 9 at the soot layer boundaries is largely due to these fluctuations.

RESULTS AND DISCUSSION

Profiles of the volume fraction of soot are shown in Fig. 3 for five liquid fuels and PMMA at a height of 4 cm above the leading edge of the fuel surface. Results from at least two different horizontal scans are shown for each fuel. Table 1 lists values of soot volume fractions, the most probable radius, and total particle concentrations at the peaks of these profiles. Since no significant change in the data occurs for wicks of different widths, errors due to the end effects are negligible. The volume fraction of soot for toluene, an

aromatic compound, is exceptionally large. Previous studies of soot formation have found that aromatics have an unusually large sooting tendency.[29] The five liquid fuels were included in tests for sooting heights by Clarke, Hunter, and Garner.[10] Their ranking of the fuels for the amount of soot formation agrees with the ranking shown in the data of Fig. 3.

Previous measurements in small pool fires[5-7,30] show the volume fraction of soot at 2 cm above the fuel surface for PMMA, iso-octane, and toluene are 0.22×10^{-6}, 0.46×10^{-6}, and 4.8×10^{-6}, respectively. The pool fire results, which are average values across the fire, lie between the maximum and minimum values of the profiles in the boundary layer.

Figures 4 through 6 present profiles of the volume fraction of soot at various heights from the leading edge of the fuel surface for n-heptane, cyclohexene, and toluene. Experimental standard deviations of f_v are shown by bars, which were obtained from standard deviations in the extinction coefficients by standard statistical techniques.[7] Bars are omitted where they would mask trends. The increase in the soot volume fraction for n-heptane is large between the heights of 2 cm and 4 cm, but the amount of increase diminishes with height. Unlike the results for n-heptane, the maximum soot volume fraction for toluene does not change significantly between the heigths of 2 cm and 4 cm (compare Figs. 3 and 6). The variations of soot volume fraction with height for cyclohexene falls between the two limiting cases of n-heptane and toluene. As the height increases the outer edge of the soot layer follows the blue flame zone away from the fuel surface, and the width of the soot layer increases. At the lower heights the

effects due to the opposing processes of formation and oxidation of soot are more apparent, causing sharply peaked f_v profiles.

From Figs. 4 and 6 soot particles are found closer to the fuel surface for toluene than n-heptane at a height of 2 cm. It is unclear if soot particles are formed closer to the wall for toluene, because convection of soot particles from upstream may transport particles to a location where they are not formed. Although the position of the inner edge of the soot layer varies between fuels, the location of the outer edge is approximately the same for all the liquid fuels. Since the thermophysical properties of these hydrocarbon fuels are similar,[31-33] the location of the flame zone is approximately the same. Figure 5 shows that profiles at different x become detectable at the same values of the similarity variable, η. This exciting result suggests that specific temperatures, fuel and product concentrations, exist at the initiation of the soot and at its burnout, since these dependent variables obey similarity; f_v itself is non-similar.

In Fig. 7 the profiles of soot volume fraction for PMMA are shown at heights of 4 cm and 10 cm above the leading edge of the fuel surface. The maximum in the profile increases only slightly with height. The distance of the flame zone from the fuel surface is less for PMMA than the liquid fuels, and the distance between the peak of the profile and the fuel surface remains approximately constant with height above 4 cm. The regression of the fuel surface at 0.2 mm/min was taken into account in the data shown in Fig. 7.

For all the fuels the most probable radius, r_{max}, is between 20 nm and 50 nm, and the particle radii do not change significantly across the soot layer. Fig. 8 presents profiles of r_{max} at 2 cm and

10 cm above the leading edge for cyclohexene. The slight increase of r_{max} with height is typical for the fuels in this study. Similar results have been obtained in pool fires.[5]

The total particle concentration, N_o, increases with height as shown in Fig. 9 for cyclohexene. Since the width of the soot layer also increases with height, the number of particles across the entire soot layer increases with height. The peaks in the particle concentration profiles correspond to peak soot volume fractions, because the particle radius is approximately constant across the layer.

CONCLUSIONS

Soot volume fractions and size distributions have been measured in a well characterized combusting boundary layer in free flow for five liquid fuels and PMMA. The ranking of fuels by soot volume fraction is preserved between small pool fires and a laminar, combusting boundary layer. A previous ranking of the fuels by their sooting heights agrees with our measurements for soot volume fractions. In the laminar boundary layer the soot volume fraction increases with height for all fuels, but for fuels with a high soot volume fraction the variation with height is small. For n-heptane the soot is observed in a narrow region on the fuel rich side of the flame front. When the width of the soot layer is compared for different liquid fuels near the leading edge, a more sooty fuel produces a wider soot layer. The convection of particles downstream widens the soot layer with height. At a height of 10 cm above the fuel leading edge the width of the soot layer is approximately constant for all the liquid fuels. Since the particle radii increase very slightly with

height, little agglomeration occurs within the layer.

In the future, the well characterized nature of this radiating, combusting boundary layer will permit anaylsis of the effects on the soot paticulates of the complex interaction among: convection due to buoyant flow and thermophoretic forces, Brownian diffusion, formation, surface growth, and oxidation. These data, along with computations of the velocity, species, and thermal fields will provide bases for soot formation modeling.

NOMENCLATURE

f_v	particulate carbon volume/flame volume
g	acceleration of gravity
Gr_x	Grashof number, $g(T_w-T_\infty)x^3/\nu_\infty{}^2T_\infty$
I	radiant intensity
L	beam pathlength through fire
m	complex index of refraction
n	real index of refraction
nk	imaginary index of refraction
N_o	total particle concentration
N(r)dr	particle concentration in the size range dr about r
Q	extinction efficiency
r	particle radius
T	temperature
x	streamwise direction coordinate
y	transverse direction coordinate

Greek

λ	wavelength
ν	kinematic viscosity
ρ	density
σ	standard deviation
τ	extinction coefficient

Subscripts

i	first wavelength
j	second wavelength

m	mean
max	most probable, i.e. at maximum in N(r)
o	incident
w	fuel surface
∞	ambient

ACKNOWLEDGEMENT

This work was supported by the U.S. Department of Energy under Contract No. W-7405-ENG-48; and by the Center for Fire Research in the U.S.D.O.C. National Bureau of Standards under Grant No. NB 80-NAG-E6839 which was administered by Lawrence Berkeley Laboratory of the University of California.

REFERENCES

1. Kim, J. S., de Ris, J., and Kroesser, F. W.: Thirteenth Symposium (International) on Combustion, p. 949, The Combustion Institute, 1971.

2. Kosden, F. J., Williams, F. A., and Buman, C.: Twelfth Symposium (International) on Combustion, p. 253, The Combustion Institute, 1969.

3. Pagni, P. J., and Shih, T. M.: Sixteenth Symposium (International) on Combustion, p. 1329, The Combustion Institute, 1976.

4. Pagni, P. J., and Bard, S.: Seventeenth Symposium (International) on Combustion, p. 1017, The Combustion Institute, 1978.

5. Bard, S., and Pagni, P. J.: ASME Journal of Heat Transfer, 103, 357, 1981.

6. Bard, S., and Pagni, P. J.: "Spatial Variation of Soot Volume Fractions in Pool Fire Diffusion Flames," submitted to Combustion and Flame

7. Bard, S.: "Diffusion Flame Particulate Volume Fractions," Ph.D. Dissertation, Mechanical Engineering Dept., University of California, Berkeley, 1980.

8. Bard, S., and Pagni, P. J.: J. Quant. Spec. Rad. Trans., 25, 453, 1981.

9. Minchin, S. T.: J. of the Inst. of Petro. Tech., 17, 102, 1931.

10. Clarke, A. E., Hunter, T. G., and Garner, F. H.: J. of the Inst. Petro. Tech., 32, 627, 1946.

11. Glassman, I., and Yaccarino, P.: Eighteenth Symposium (International) on Combustion, p. 1175, The Combustion Institute, 1981.

12. Markstein, G. H.: Seventeenth Symposium (International) on Combustion, p. 1053, The Combustion Institute, 1978.

13. Jagoda, I. J., Prado, G., and Lahaye, J.: Combustion and Flame, 37, 261, 1980.

14. Kent, J. H., Jander, H., and Wagner, H. Gg.: Eighteenth Symposium (International) on Combustion, p. 1117, The Combustion Institute, 1980.

15. Haynes, B. S., and Wagner, H. Gg.: Ber. Bunsenges. Phys. Chem., 84, 499, 1980.

16. Haynes, B. S., Jander, H., and Wagner, H. Gg.: Ber. Bunsenges. Phys. Chem., 84, 585, 1980.

17. Chang, P. H. P. and Penner, S. S.: J. Quant. Spectrosc. Radiat. Transfer, 25, 105, 1981.

18. Sibulkin, M., Kulkarni, A. K., Annamalai, K.: Eighteenth Symposium (International) on Combustion, p. 611, The Combustion Institute, 1980.

19. Liu, C. N., and Shih, T. M.: ASME Journal of Heat Transfer, 102, 724, 1980.

20. Kinoshita, C. M., and Pagni, P. J.: Eighteenth Symposium (International) on Combustion, p. 1415, The Combustion Institute, 1980.

21. Beier, R. A. and Pagni, P. J.: "Radiation in Laminar Combusting Boundary Layers," submitted to Combustion and Flame

22. Beier, R. A.: "Soot and Radiation in Combusting Boundary Layers," Ph.D. Thesis, Mechanical Engineering Dept., University of California, Berkeley, 1982.

23. Kerker, M.: The Scattering of Light and Other Electomagnetic Radiation, Academic Press, 1969.

24. Lee, S. C., and Tien, C. L.: Eighteenth Symposium (International) on Combustion, p. 1159, The Combustion Institute, 1980.

25. Dalzell, W. H., and Sarofim, A. F.: ASME J. of Heat Transfer, 91, 100, 1969.

26. Hahn, G. H., and Shapiro, S. S.: Statistical Models in Engineering, John Wiley and Sons, New York, 1968.

27. Westborg, G. H., Howard, J. B., and Williams, G. C.: Fourteenth Symposium (International) on Combustion, p. 929, The Combustion Institute, 1973.

28. Lee, S. C., and Tien, C. L.: "Thermal Radiation of Spherical and Cylindrical Soot Particles," Paper No. 80-54, Western States Section of the Combustion Institute, Fall Meeting, 1980.

29. Bittner, J. D., and Howard, J. B.: "Role of Aromatics in Soot Formation," in Alternative Hydrocarbon Fuels: Combustion and Kinetics, Progress in Astronautics and Aeronautics, Vol. 62, pp. 335-358, Amer. Inst. of Aero. and Astro., New York, 1978.

30. Lee, S. C.: "Soot Radiation from Diffusion Flames," Ph.D. Dissertation, Mechanical Engineering Dept., University of California, Berkeley, 1981.

31. Perry, J. H.: Chemical Engineers' Handbook, McGraw-Hill, New York, 1975.

32. Obert, E. F.: Internal Combustion Engines, International Textbook Co., Scranton, Penn., 1968.

33. Varaftik, N. B.: Tables of Thermophysical Properties of Liquids and Gases, Hemisphere Publishing Corp., distributed by John Wiley, 1975.

Table 1. Summary of Peak Soot Volume Fractions and Size Distributions at x = 4 cm.

Fuel	Sample Width (cm)	Wavelength Pair, i-j	Path-length L (cm)	Distance from Fuel Surface (mm)	$(I/I_o)_i$	$(I/I_o)_j$	$f_v \times 10^{-6}$	r_{max} (nm)	$N_o \times 10^{-9}$ (cm^{-3})
Liquids									
Toluene (C_7H_8)	3	1-4	3.3	3.2	0.0043	0.028	10	44	6.3
	3	2-4	3.2	3.5	0.0012	0.0096	13	45	7.2
Cyclohexene (C_6H_{10})	7	1-4	8.2	4.6	0.039	0.17	2.1	32	3.5
	7	2-4	8.2	4.4	0.10	0.25	1.9	31	3.5
Iso-octane (C_8H_{18})	3	1-4	3.7	4.8	0.52	0.69	1.0	36	1.2
	7	1-4	7.7	4.8	0.21	0.46	1.3	25	4.5
	15	1-4	16.0	4.8	0.063	0.24	1.1	27	3.0
	15	2-4	16.0	4.5	0.088	0.23	1.0	31	1.8
	15	3-4	16.0	4.8	0.11	0.23	1.1	27	3.0
Cyclohexane (C_6H_{12})	7	1-4	7.9	4.1	0.37	0.58	0.70	33	1.1
	15	1-4	16.1	4.1	0.15	0.35	0.67	32	1.1
n-Heptane (C_7H_{16})	7	1-4	8.3	4.0	0.54	0.73	0.43	28	1.0
	15	1-4	16.2	4.4	0.27	0.51	0.49	27	1.3
	15	2-4	16.2	4.6	0.39	0.55	0.36	35	0.46
Solid									
Polymethyl-methacrylate $(C_5H_8O_2)_n$	16	1-4	15.8	2.3	0.38	0.63	0.39	23	1.7

FIGURE CAPTIONS

Fig. 1. Schematic diagram of a steady, two dimensional, laminar, combusting, boundary layer on a pyrolyzing fuel slab.

Fig. 2. Schematic diagram of apparatus for simultaneous multi-wavelength laser transmission measurements.

$L\lambda_i$, $L\lambda_j$	- Laser at λ_i or λ_j
M	- Mirror
B	- Beamsplitter
P	- Prism
FL1	- Focusing lens #1 (f = 550 mm)
FL2	- Focusing lens #2 (f = 250 mm)
FL3	- Focusing lens #3 (f = 200 mm)
FL4	- Focusing lens #4 (f = 78 mm)
F	- Bandpass filter (bandwidth = 30 A)
$DT\lambda_i$, $DT\lambda_j$	- Detector for transmitted intensity
$DR\lambda_i$, $DR\lambda_j$	- Detector for reference intensity
OS	- Output signal to amplifier and computer

Fig. 3. Soot volume fraction, f_v, as a function of distance from the fuel surface at a height of 40 mm for five liquid, hydrocarbon fuels and PMMA.

Fig. 4. Soot volume fraction, f_v, as a function of distance from fuel surface at different heights for n-heptane. Wavelength pair numbers refer to λ_i . (λ_1 = 0.4579 m, λ_2 = 0.4880 m, λ_3 = 0.5145 m, λ_4 = 0.6328 m).

Symbol	x (mm)	Wavelength Pair
△	20	1-4
□	20	2-4
▽	40	1-4
◇	40	2-4
▼	100	1-4
◆	100	2-4
▲	100	3-4

Fig. 5. Soot volume fraction, f_v, as a function of a similarity transformation coordinate or distance from the fuel surface at different heights for cyclohexene. The symbol definitions are those given in caption to Fig. 4.

Fig. 6. Soot volume fraction, f_v, as a function of distance from the fuel surface at x = 2 cm for toluene. The symbol definitions are those given in the caption of Fig. 4.

Fig. 7. Soot volume fractions, f_v, for PMMA as a function of distance from the fuel surface at different heights. The symbol definitions are those given in the caption to Fig. 4.

Fig. 8. Most probable radius, r_{max}, as a function of distance from the fuel surface at different heights for cyclohexene. The symbol definitions are those given in the caption to Fig. 4.

Fig. 9. Total particle concentration, N_o, as a function of distance from the fuel surface at different heights for cyclohexene in free flow. The symbol definitions are those given in the caption of Fig. 4.

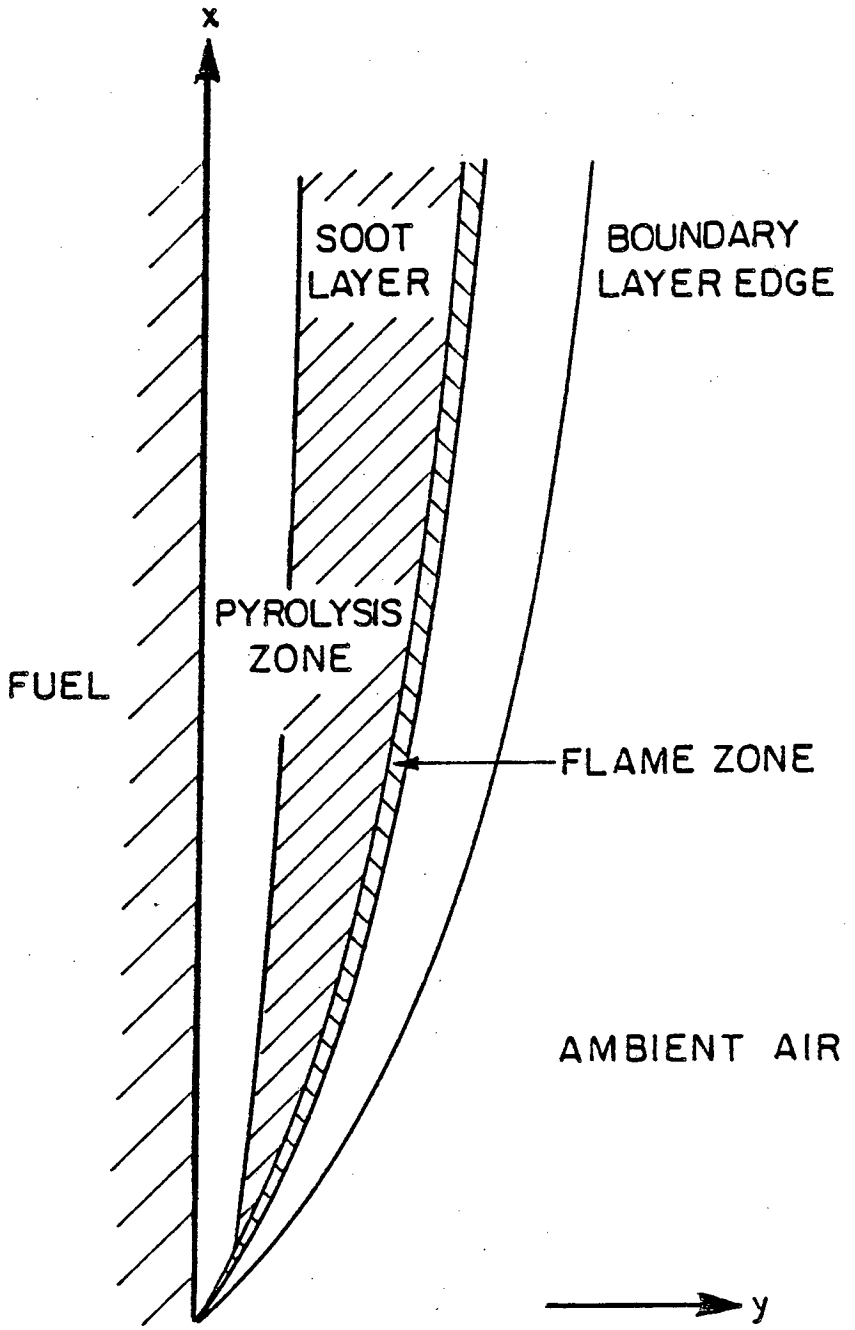

Fig. 1

XBL813-5397

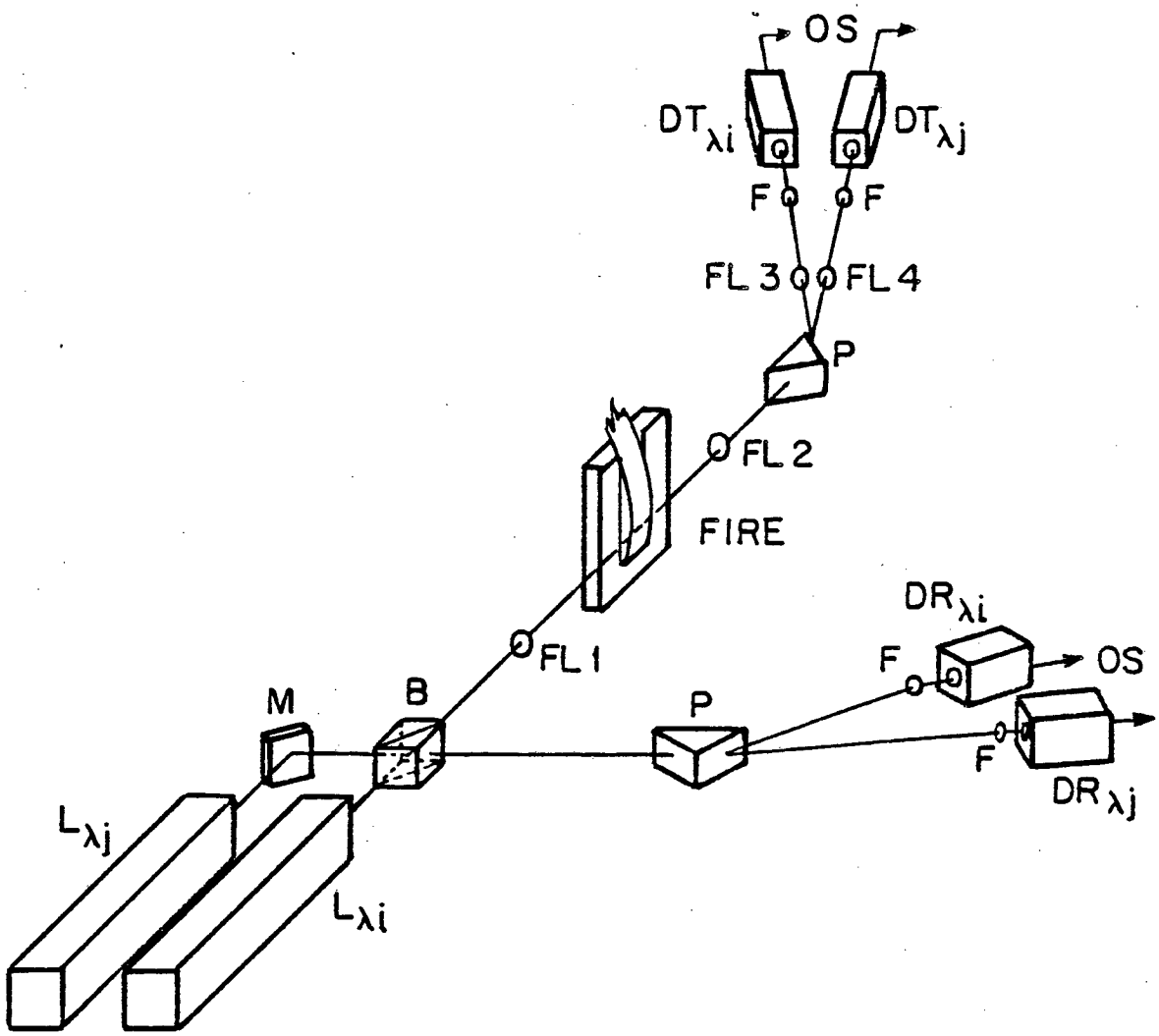

Fig. 2

XBL813-5398

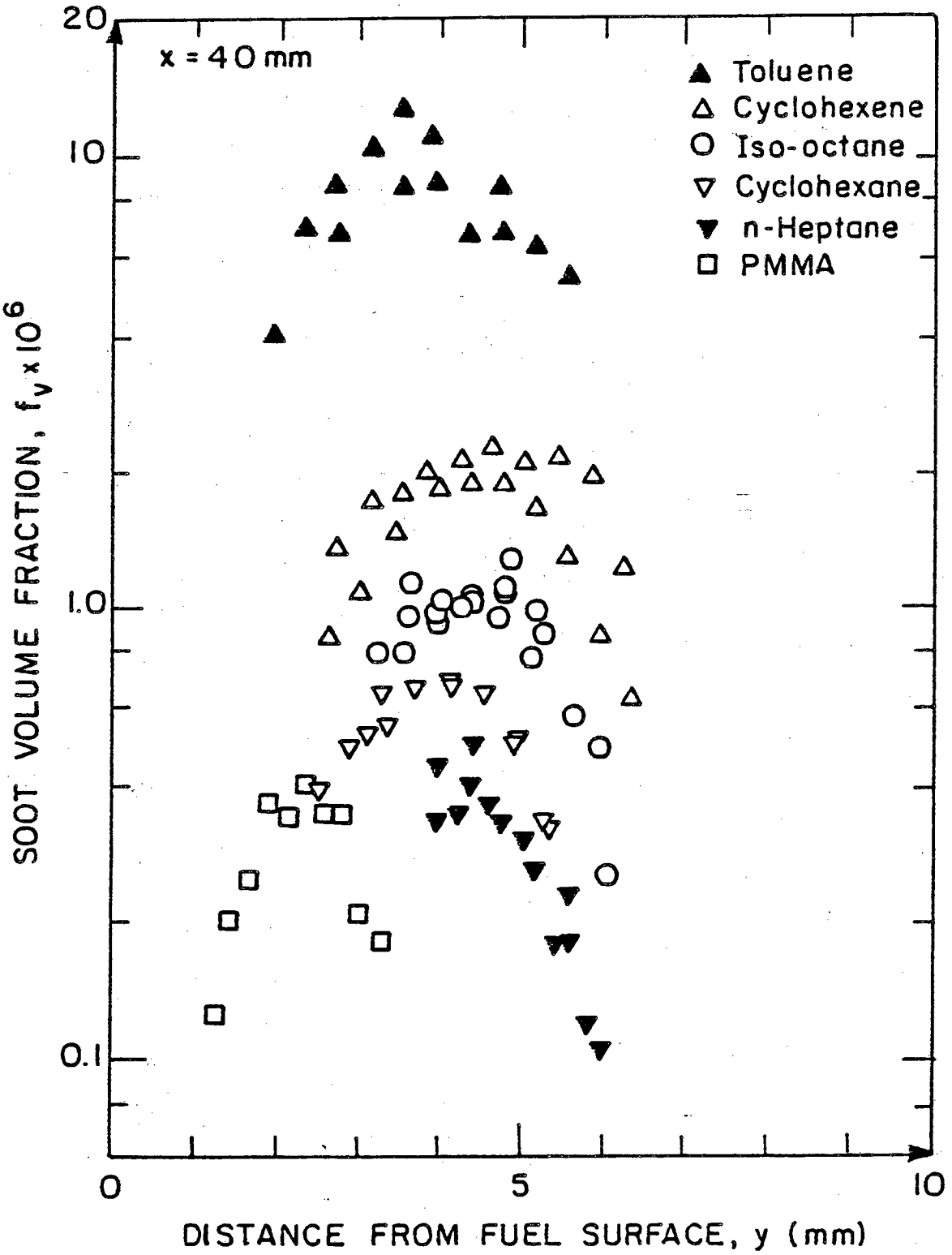

Fig. 3

XBL 813-5399

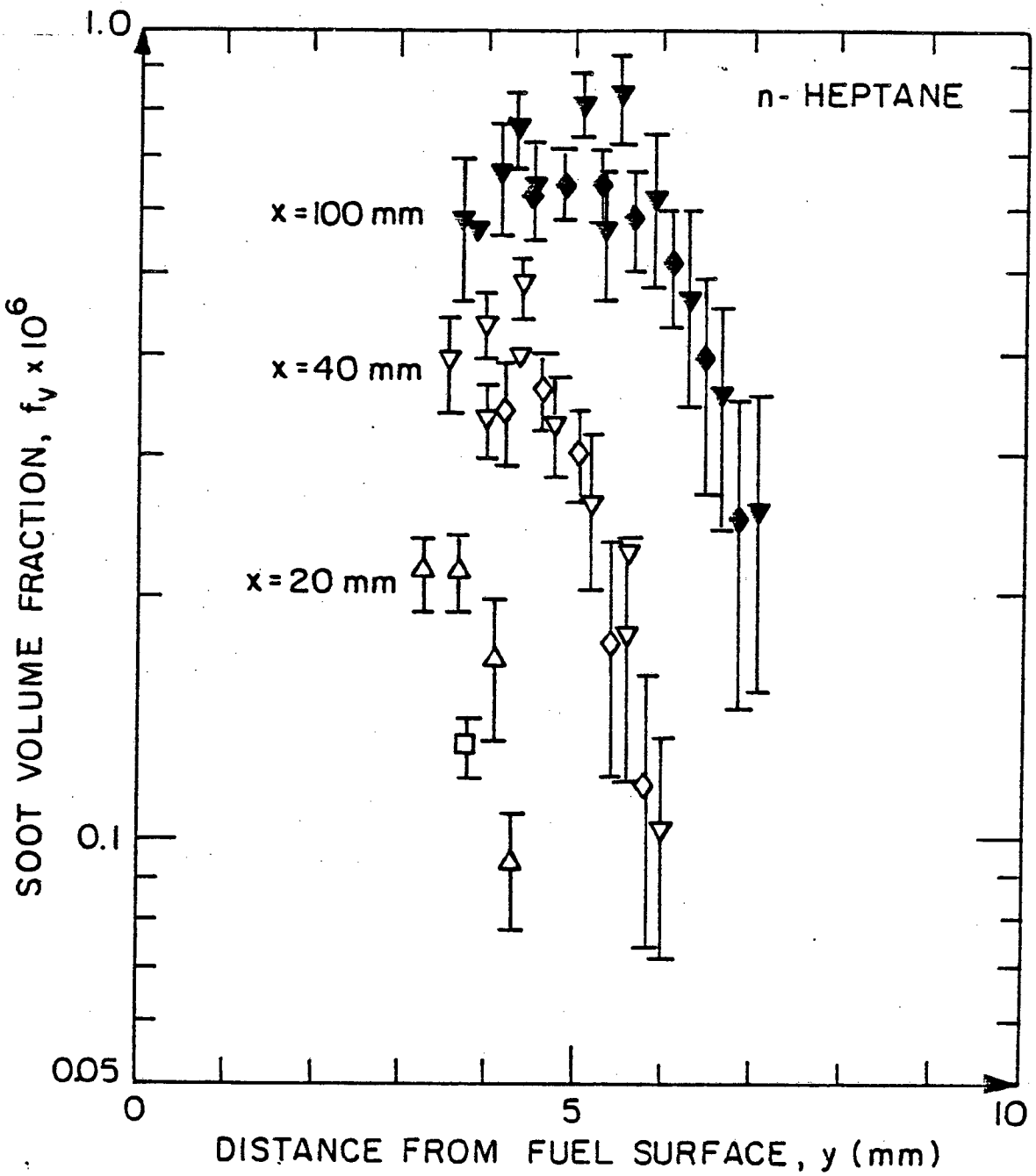

Fig. 4

XBL 813-5400

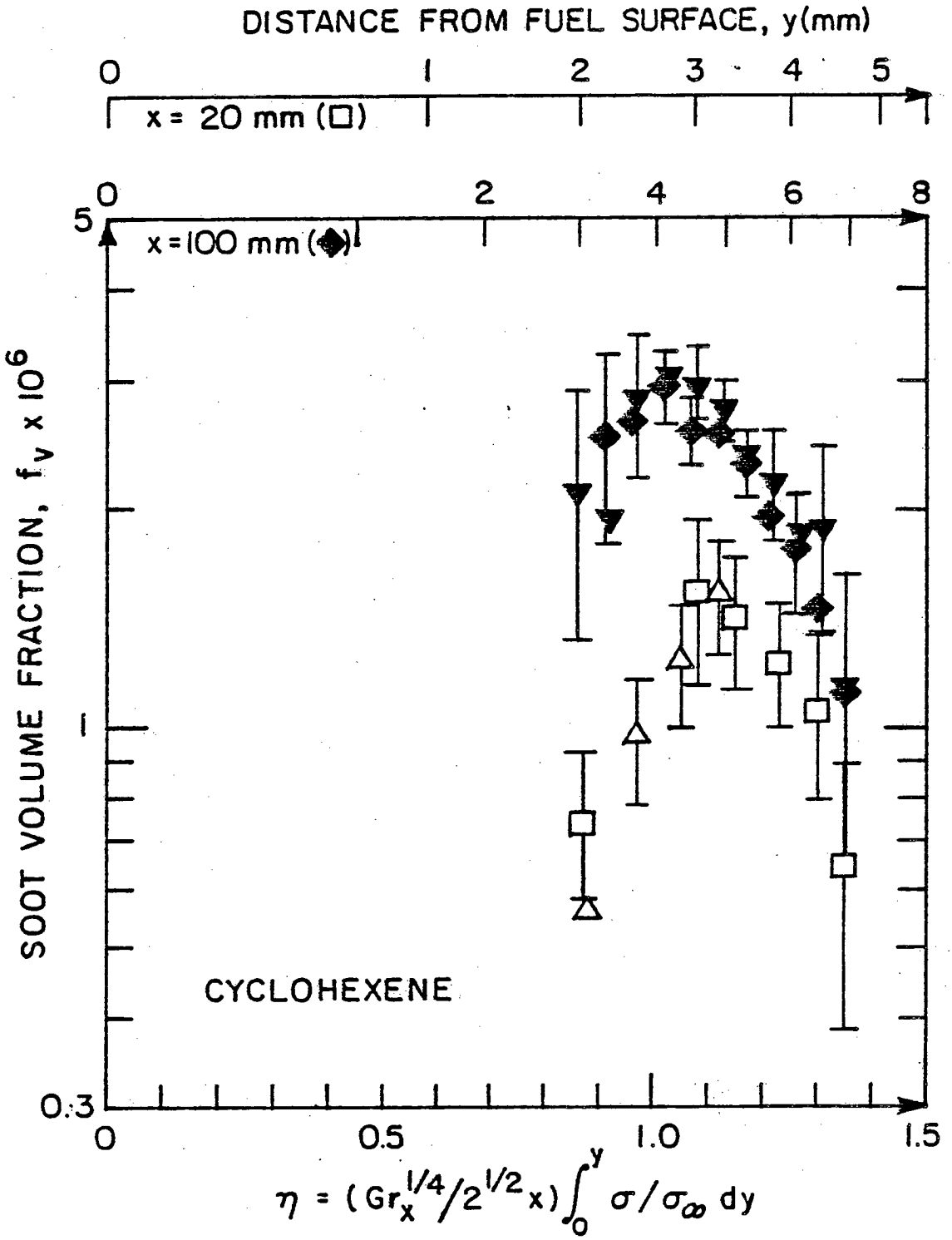

Fig. 5

XBL 8112-13188

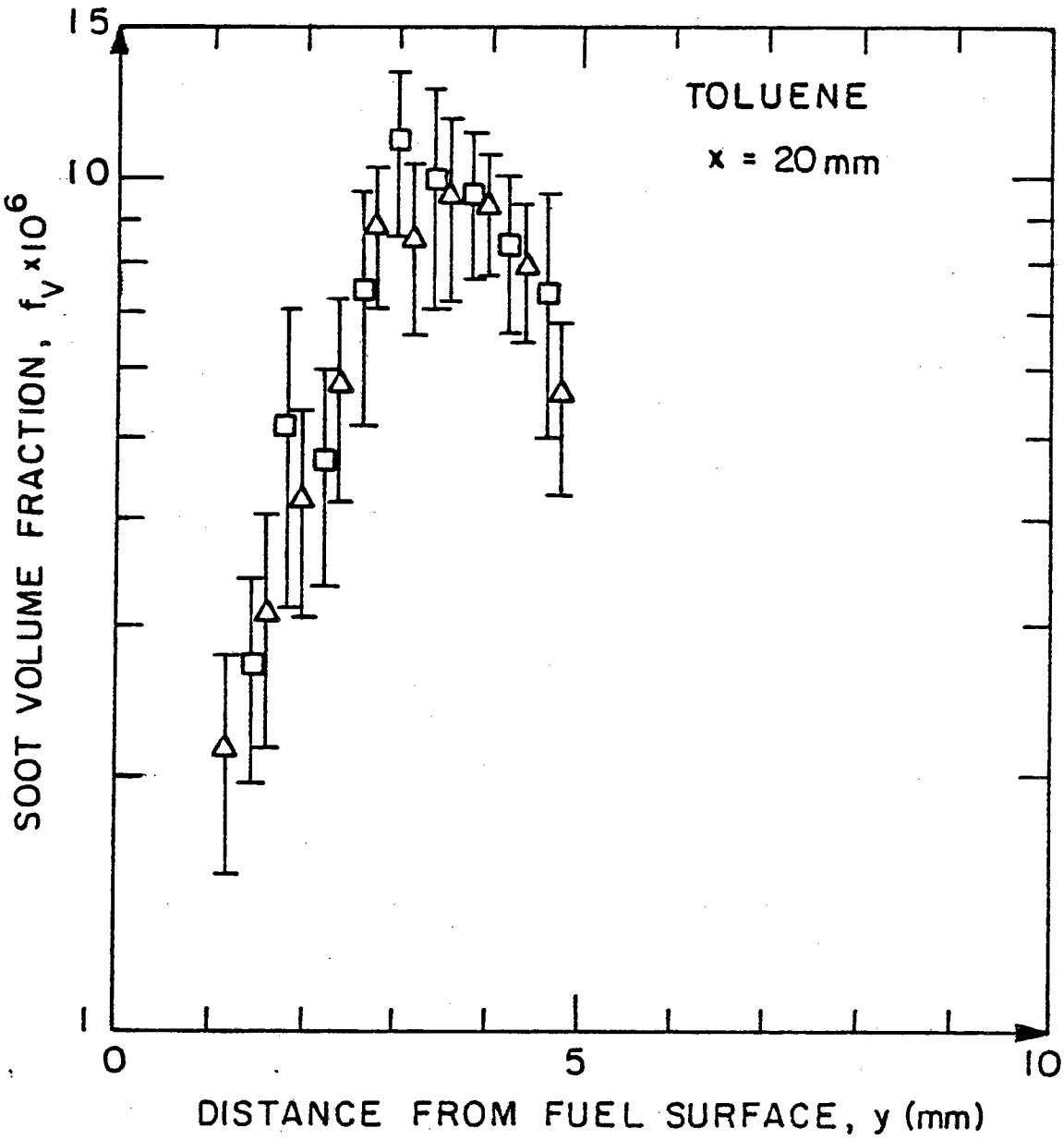

Fig. 6

XBL 813-5402

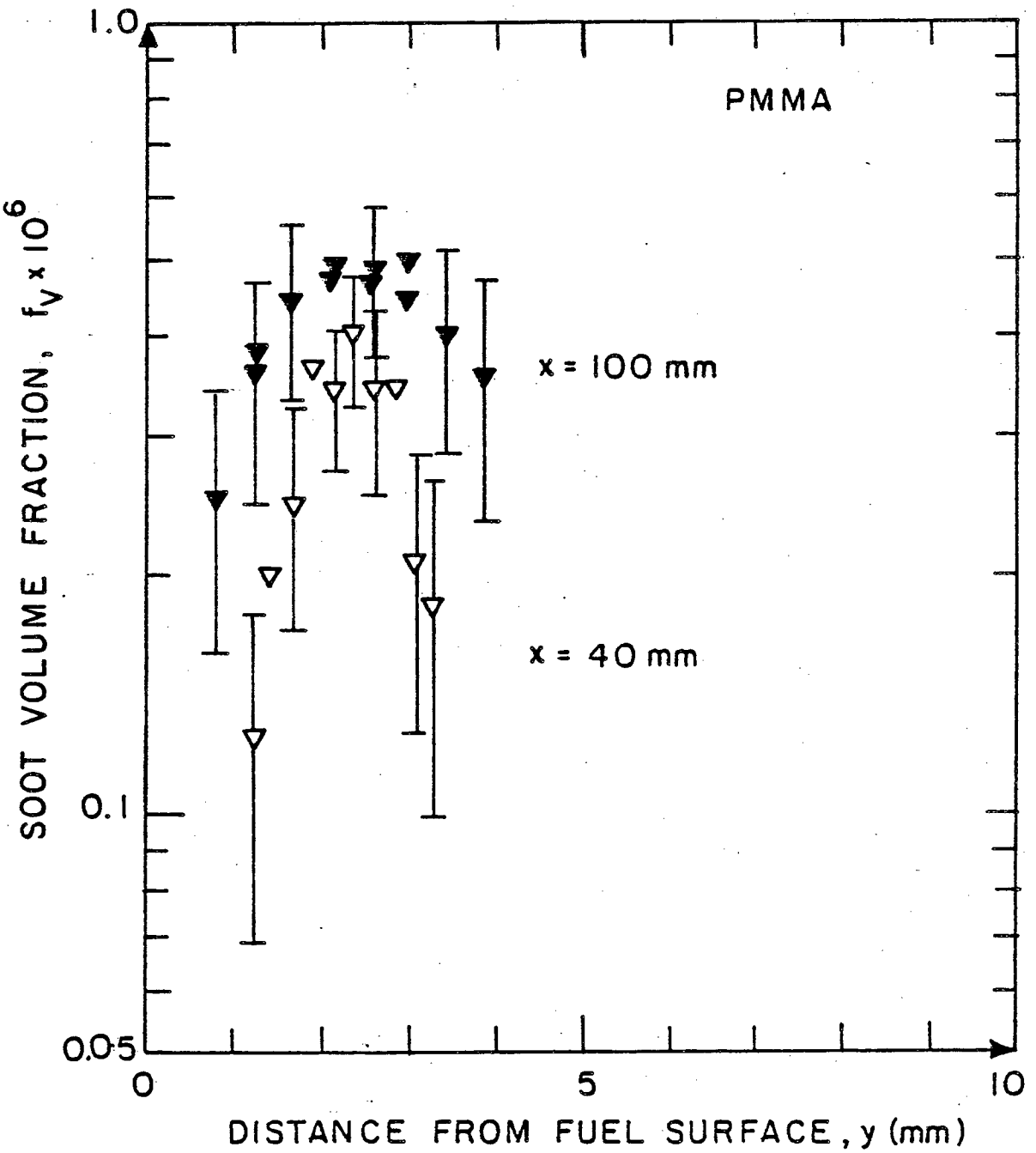

Fig. 7

XBL 813-5403

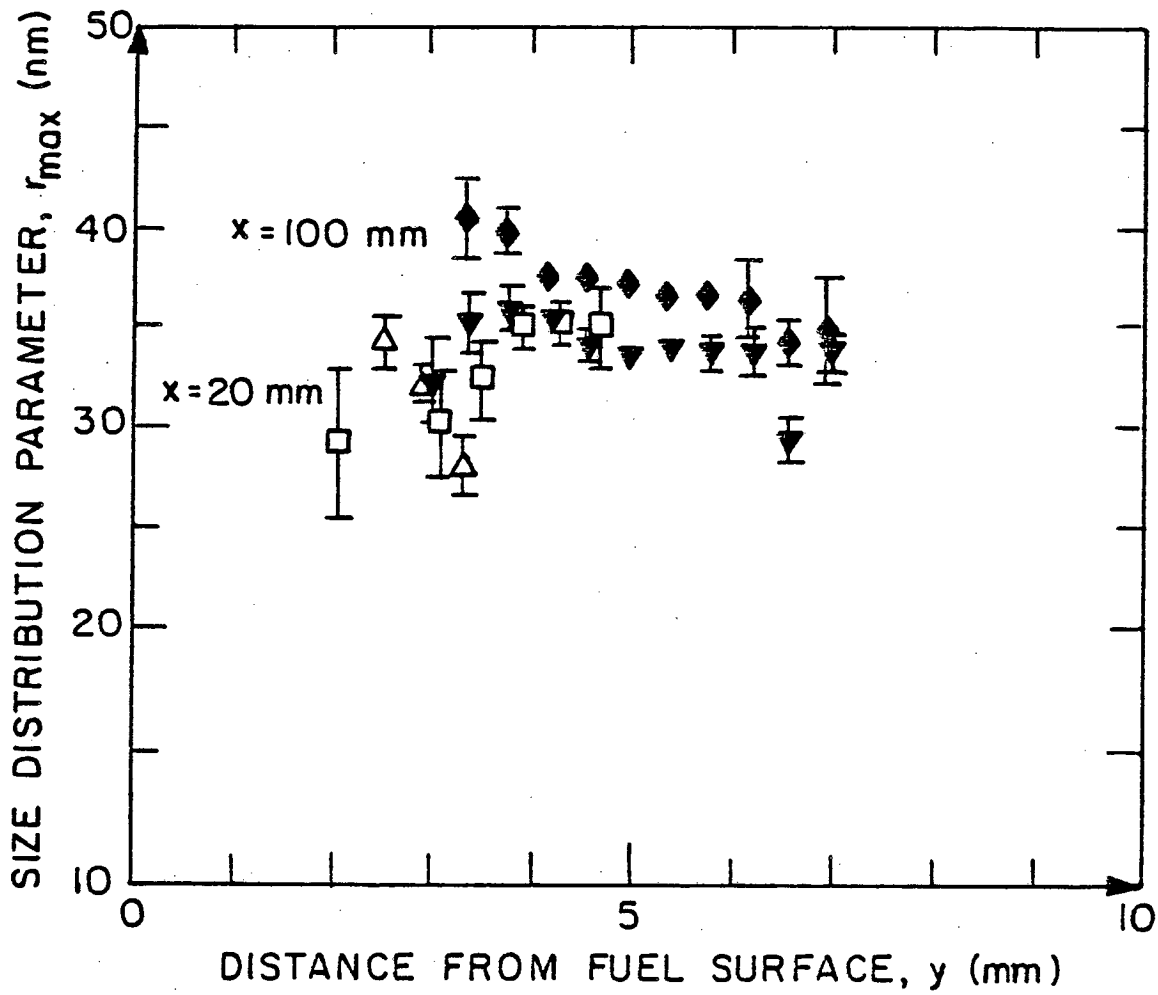

Fig. 8

XBL813-5404

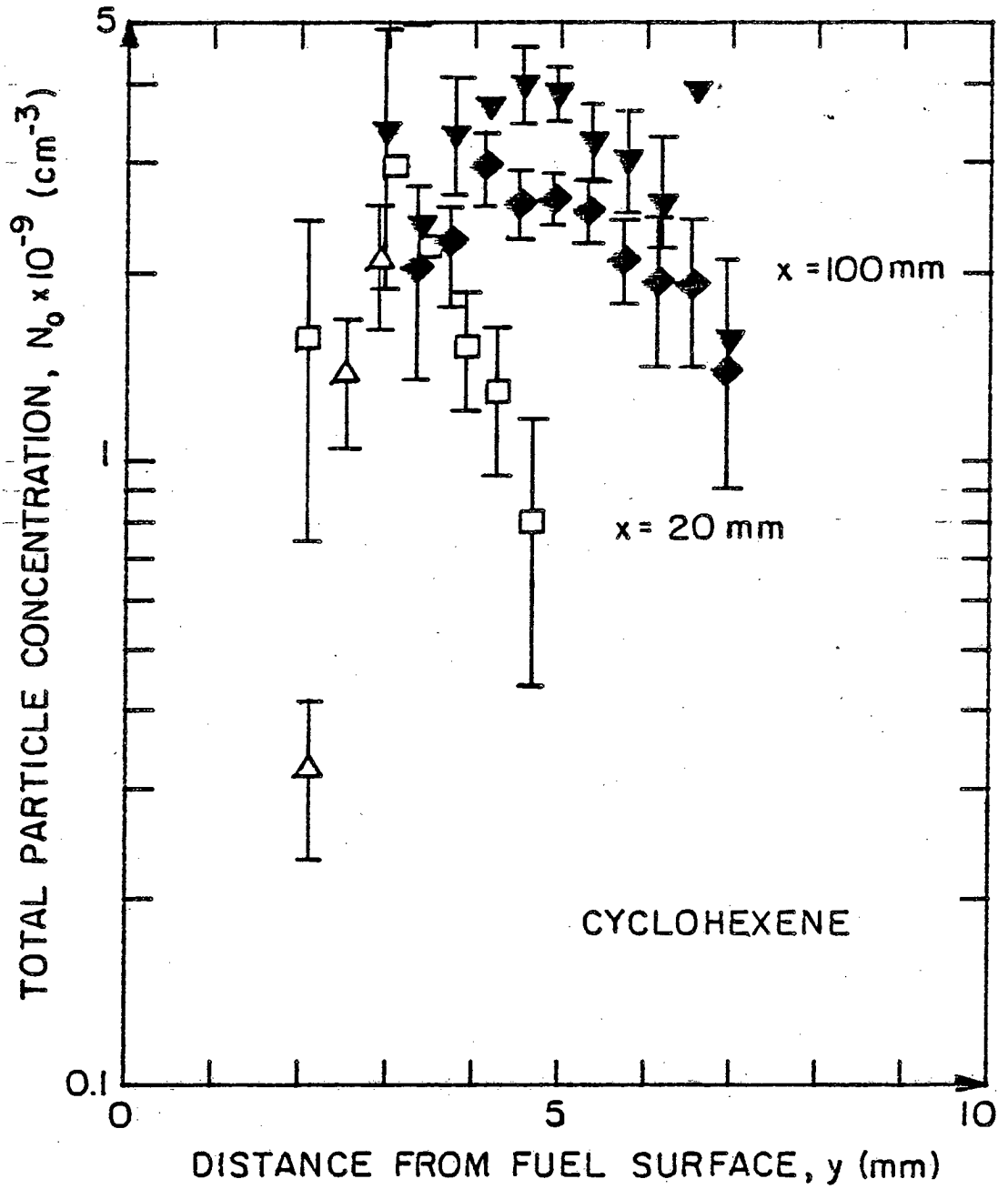

Fig. 9

XBL8111-12810

TECHNICAL INFORMATION DEPARTMENT
LAWRENCE BERKELEY LABORATORY
UNIVERSITY OF CALIFORNIA
BERKELEY, CALIFORNIA 94720